PHYSICAL REVIEW B VOLUME 22, NUMBER 12 15 DECEMBER 1980

Phonons in solid argon

H. R. Glyde and M. G. Smoes
Department of Physics, University of Ottawa, Ottawa, Canada K1N 6N5
(Received 3 April 1980)

The phonon energies and the dynamic form factor, $S(\vec{Q},\omega)$, in solid ^{36}Ar at temperatures from 10 K to the melting point are calculated using the self-consistent-phonon (SCP) theory with the pair interaction represented by the recent realistic potential developed by Aziz and Chen. The temperature dependence of the phonon energies agree well with the observed values of Fujii *et al.* This is a substantial improvement over the previously available calculations obtained using anharmonic perturbation theory. The temperature broadening of $S(\vec{Q},\omega)$ also agrees well with the observed phonon groups for low-energy phonons where data are available and with the molecular dynamics (MD) calculations of Hansen and Klein. The $S(\vec{Q},\omega)$ for high-energy phonons near melting are found to be extremely broad, broader than in solid helium, and $S(\vec{Q},\omega)$ becomes very sensitive to intermediate phonon energies used in its calculation, making the present SCP group shapes not reliable for high-energy phonons near melting. Further experimental data or MD simulation of $S(\vec{Q},\omega)$ near melting for high-energy phonons would be most useful as a test of anharmonic theory, for example, of whether an explicit description of short-range correlations in the atomic motion is important.

I. INTRODUCTION

The dynamical properties of solid argon have a long and rich history[1] of study. This is because the potential of the solid can be well represented[2] by a sum of pair interactions between argon atoms with the addition of the Axilrod-Teller-Muto (ATM) triple-dipole interaction. Comparison of theory with experiment then represents a reliable test of our understanding of the dynamics.

Prior to the pioneering measurements of phonon energies and lifetimes using inelastic neutron scattering by Daniels *et al.*[3] in solid krypton and by Egger *et al.*,[4] Batchelder *et al.*,[5] and Fujii *et al.*[6] in solid ^{36}Ar, the early work on solid argon focused mainly on the elastic and thermodynamic properties. This work, both theory and properties, is elegantly reviewed by Dobbs and Jones,[7] Pollack,[8] Boato,[9] Guggenheim,[10] and Horton.[11] The calculations of Horton and Leech[12] and the review by Horton[11] stand out as the early detailed discussion of the phonon frequency dispersion curves. In all these studies the pair interaction was represented by a model pair potential, generally of the Mie and Lennard-Jones type.

The first detailed calculation of the phonon frequencies and lifetimes in solid argon over a wide temperature range was by Bohlin and Högberg[13] who used quasiharmonic theory with a perturbation treatment of the quartic and cubic anharmonic terms (QHPT). Niklasson[14] also used the QHPT to calculate phonon properties in argon and both he and Bohlin and Högberg employed the Lennard-Jones potential.

The first calculations in solid argon using realistic pair potentials appeared in a series of papers by Bobetic and Barker (BB),[15] Barker *et al.*,[16] and Klein *et al.*[17] They employed a potential developed by Bobetic and Barker to represent the pair argon interaction and the ATM potential to represent the three-body interactions. For calculating phonon frequencies this potential is indistinguishable[18] from the more widely known and accurate Barker-Fisher-Watts[19] potential although some difference can be seen in the expansivity. With this potential and using the QHPT Bobetic and Barker[15] and Barker *et al.*[16] obtained elastic constants and phonon frequencies in good agreement with the observed values near 0 K. However, Klein *et al.*[17] found the temperature dependence of these QHPT frequencies agreed poorly with the temperature dependence observed by Batchelder *et al.*[5] This was not improved when the QHPT was replaced by the self-consistent harmonic approximation.

Goldman *et al.*[20] calculated the phonon dispersion curves at 0 K using a more complete self-consistent theory and the Lennard-Jones potential and also found good agreement with the observed phonon energies at 0 K available at that time. Using the powerful molecular dynamics (MD) method, Hansen and Klein[21] evaluated directly the dynamic form factor $S(\vec{Q},\omega)$ in a "Lennard-Jones solid." They found significant differences between their "exact" $S(\vec{Q},\omega)$ and that calculated using the self-consistent-phonon (SCP) theory for selected phonons at high temperature. An exhaustive review of all the dynamic and thermodynamic properties of all the rare-gas crystals has been made by Klein and Koehler.[18]

In this context we have evaluated the phonon frequencies and $S(\vec{Q},\omega)$ in solid ^{36}Ar at all temperatures using the self-consistent-phonon theory and the recent realistic potential developed by Aziz and Chen. The Aziz-Chen potential is shown in Fig. 1.

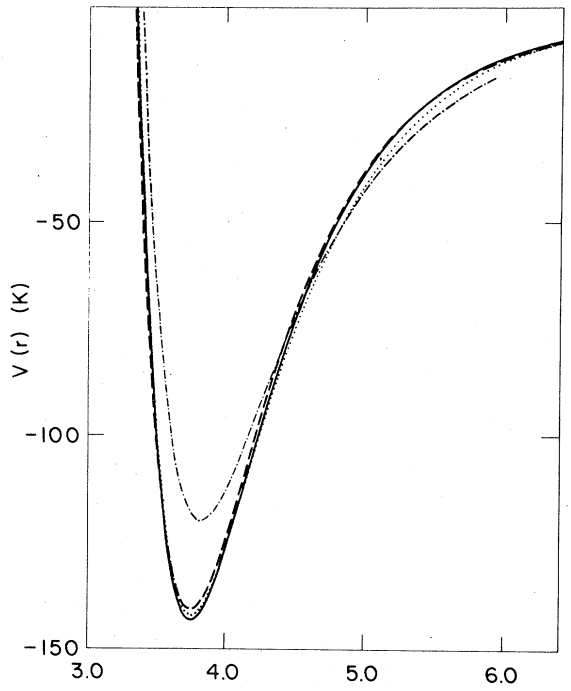

FIG. 1. Argon pair potential in the well region: —— Aziz-Chen (Ref. 22), ··· Barker-Fisher-Watts (Ref. 19), --- Parson-Siska-Lee (Ref. 35), and -·- Lennard-Jones.

The results are compared with the more recent and accurate neutron scattering data of Fujii *et al.* and the MD studies of Hansen and Klein. The aim is to test whether the temperature dependence of the phonon frequencies and the temperature broadening of $S(\vec{Q},\omega)$ can be correctly predicted. This will help answer (1) whether at high temperature the SCP theory is a substantial improvement over the QHPT and (2) whether the SCP theory itself is reliable at high temperatures. Since the role of the ATM forces has been clearly established by Barker *et al.*, we do not include them in the calculation of the phonon frequencies here. Their contribution to the frequencies is discussed in Sec. III.

The technical details of the present calculations are outlined in Sec. II and the low-temperature results are presented in Sec. III. The temperature dependence of the phonon frequencies and the dynamic form factors are presented in Secs. IV and V. The results are discussed in Sec. VI.

II. THE SELF-CONSISTENT THEORY

A. Dynamic form factor

The cross section for the coherent scattering of neutrons from a solid is proportional to the dynamic form factor,[23]

$$S(\vec{Q},\omega)=\int dt\, e^{i\omega t}\frac{1}{N}\sum_{ll'} e^{i\vec{Q}\cdot(\vec{R}_l-\vec{R}_{l'})} \times\langle e^{i\vec{Q}\cdot\vec{u}_l(t)}e^{-i\vec{Q}\cdot\vec{u}_{l'}(0)}\rangle . \quad (1)$$

Here $\vec{Q}$ is the wave vector of the excitation created by the neutron and $\hbar\omega$ is the energy transferred from the neutron to the solid. The $S(\vec{Q},\omega)$ is then expanded in powers of the displacements $\vec{u}_l$ of atoms l from their lattice points $\vec{R}_l$ and, ignoring the elastic Bragg scattering component,

$$S(\vec{Q},\omega)=S_1(\vec{Q},\omega)+S_{12}(\vec{Q},\omega)+S_2(\vec{Q},\omega)+\cdots . \quad (2)$$

The $S_1(\vec{Q},\omega)$, proportional to $\langle[\vec{Q}\cdot\vec{u}]^2\rangle$, describes the scattering in which the excitation is a single phonon having wave vector $\vec{q}=\vec{Q}$. The $S_2(\vec{Q},\omega)$, proportional to $\langle(\vec{Q}\cdot\vec{u})^4\rangle$, describes the scattering process in which two phonons are created (or destroyed) and $S_{12}(\vec{Q},\omega)$ represents the interference contribution between the scattering from one- and two-phonon processes. The higher-order processes we hope should be small or at least uniform, uninteresting functions of ω.

B. Phonon dynamics

The one-phonon $S_1(\vec{Q},\omega)$ is[23-25]

$$S_1(\vec{Q},\omega)=[n(\omega)+1]d^2(Q)\sum_{\lambda}(\vec{Q}\cdot\vec{\epsilon}_{q\lambda})^2 \times f_{q\lambda}^2 A(q\lambda,\omega)\Delta(\vec{Q}-q) . \quad (3)$$

Here $n(\omega)$ is the Bose function, $d(Q)$ is the Debye-Waller factor, $f_{q\lambda}^2=(\hbar/2m\omega_{q\lambda})$, $\vec{\epsilon}_{q\lambda}$ and $\omega_{q\lambda}$ are the polarization and frequency of the phonon having branch λ, and m is the atomic mass.

In the self-consistent harmonic (SCH) approximation, the $\omega_{q\lambda}$ are given by the usual harmonic expression,[26]

$$\omega_{q\lambda}^2=\vec{\epsilon}_{q\lambda}\frac{1}{m}\sum_{l}{}'(e^{i\vec{q}\cdot\vec{R}_{0l}}-1)\langle\vec{\nabla}(0)\cdot\vec{\nabla}(l)v(r_{0l})\rangle\vec{\epsilon}_{q\lambda} \quad (4)$$

in which the force constants $\langle\vec{\nabla}(0)\cdot\vec{\nabla}(l)v(r_{0l})\rangle$ are evaluated as derivatives of the interatomic potential $v(r_{0l})$ averaged over the vibrational distribution of the atoms about their lattice points. The vibrational distribution is described by a Gaussian function of rms amplitude $\langle\vec{u}_l^2\rangle$ consistent with the SCH frequencies,

$$\langle u_l^2\rangle=\sum_{q\lambda}f_{q\lambda}^2[2n(\omega_{q\lambda})+1] .$$

In the SCH theory in which the cubic anharmonic term is added as a perturbation[27] (SCH + C) the one-phonon response function in $S_1(Q,\omega)$ takes the usual anharmonic form,[24]

$$A(q\lambda,\omega)=\frac{8\omega_{q\lambda}^2\Gamma(q\lambda,\omega)}{[-\omega^2+\omega_{q\lambda}^2+2\omega_{q\lambda}\Delta(q\lambda,\omega)]^2+[2\omega_{q\lambda}\Gamma(q\lambda,\omega)]^2}. \tag{5}$$

The Δ and Γ are the phonon frequency shift and inverse lifetime due to the cubic anharmonic term[24,27]

$$\Delta(q\lambda,\omega)=-(2\hbar^2)^{-1}\sum_{1,2}|V(q\lambda,1,2)|^2M(1,2,\omega), \tag{6}$$

$$\Gamma(q\lambda,\omega)=-(2\hbar^2)^{-1}\sum_{1,2}|V(q\lambda,1,2)|^2J(1,2,\omega),$$

where

$$M(1,2,\omega)=(n_1+n_2+1)\left(\frac{1}{\omega+\omega_1+\omega_2}-\frac{1}{\omega-(\omega_1+\omega_2)}\right)$$
$$-(n_2-n_1)\left(\frac{1}{\omega+\omega_2-\omega_1}-\frac{1}{\omega-\omega_2+\omega_1}\right)$$

and (7)

$$J(1,2,\omega)=(n_1+n_2+1)\pi[\delta(\omega-(\omega_1+\omega_2))-\delta(\omega+\omega_1+\omega_2)]$$
$$+(n_2-n_1)\pi[\delta(\omega+\omega_2-\omega_1)-\delta(\omega-\omega_2+\omega_1)],$$

where $\omega_1=\omega_{q_1\lambda_1}$ and $n_1=n(\omega_1)$ and so on. In these expressions $V(\vec{q}\lambda,1,2)$ is essentially the Fourier transform of $\langle\vec{\nabla}(0)\cdot\vec{\nabla}(0)\cdot\vec{\nabla}(l)v(r_{0l})\rangle$, the third derivative of $v(r_{0l})$ averaged over the same vibrational distribution as appearing in (4). If $\Delta(\vec{q}\lambda,\omega)$ and $\Gamma(\vec{q}\lambda,\omega)$ depend little on frequency, then $A(\vec{q}\lambda,\omega)$ is a simple Lorentzian function peaking at $\omega^2=\omega_{q\lambda}^2+2\omega_{q\lambda}\Delta(\vec{q}\lambda,\omega)$ with a full width at half maximum FWHM of $W\simeq 2\Gamma(\vec{q}\lambda,\omega)$. The position of this peak is usually identified as the SCH + C phonon frequency.

For harmoniclike phonons,

$$S_2(\vec{Q},\omega)=[n(\omega)+1]d^2(Q)\times\frac{1}{N}\sum_{12}f_1^2(\vec{Q}\cdot\vec{\epsilon}_1)^2f_2^2(\vec{Q}\cdot\vec{\epsilon}_2)^2\times J(1,2,\omega)\Delta(\vec{Q}-(\vec{q}_1+\vec{q}_2)). \tag{8}$$

Here $J(1,2,\omega)$ given in (7) is usually referred to as the two-phonon density of states. Since in $S_2(\vec{Q},\omega)$ there is a sum over all phonons having wave vector $\vec{q}_1$ [with $\vec{q}_2$ fixed by $\Delta(\vec{Q}-(\vec{q}_1+\vec{q}_2))$] we expect $S_2(\vec{Q},\omega)$ to be a reasonably uniform function of ω. The interference term, $S_{12}(\vec{Q},\omega)$, has been discussed extensively[25,28-33] and we do not discuss it here.

III. PHONONS AT LOW TEMPERATURE

In ^{36}Ar at low temperature ($T\leq 10$ K), where anharmonic effects are small and we may be reasonably confident of the dynamics, we may compare the calculated phonon frequencies and elastic constants with experiment as a test of the interatomic potential. In Fig. 2 we compare the phonon frequencies calculated using the SCH + C approximation and the Aziz-Chen potential with the observed values of Fujii *et al.* There we see the overall agreement is excellent, especially for the transverse branches. The SCH + C longitudinal frequencies do, however, lie definitely above the observed values for wave vectors at the Brillouin-zone edge. The SCH + C longitudinal frequencies lie below the observed values at small wave vector.

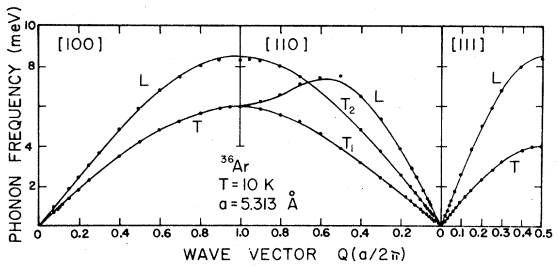

FIG. 2. Phonon energies calculated in the SCH+ C approximation (solid line) and observed by Fujii *et al.* (Ref. 6) (points).

Barker *et al.*[16] and Klein *et al.*[17] have calculated the phonon frequencies at 0 K and higher temperatures, respectively, using quasiharmonic perturbation theory (QHPT). They described the pair potential using the Bobetic-Barker form (a slightly extended Barker-Pompe potential) and included the three-body, triple-dipole Axilrod-Teller-Muto (ATM) forces. Their transverse phonon frequencies at 0 and 4 K are indistinguishable from the present results and experiment. This is demonstrated in Table I where some selected transverse phonon energies are compared. Their longitudinal frequencies lie above the present SCH + C results, due to the addition of the three-body forces, and therefore agree better with experiment at low q but less well at high q.

TABLE I. The phonon energies (meV) for selected transverse phonons along the $[\xi 00]$ direction in ^{36}Ar at $T=10$ K (AC means Aziz-Chen potential). The QHPT BB are the values calculated by Klein *et al.* using quasiharmonic perturbation theory and the Bobetic-Barker potential at $T=4$ K. The observed values are from Fujii *et al.* (Ref. 6).

ξ	SCH + C AC potential	QHPT BB potential	Obs.	QH AC potential	QH LJ potential
0.4	3.47	3.47	3.46±0.01	3.35	3.29
0.7	5.24	5.25	5.25±0.01	5.07	4.97
1.0	5.90	5.91	5.94±0.03	5.69	5.58

TABLE II. Elastic constants c_{ij} of Ar at $T=10$ K in 10^8 dynes/cm^2, $\delta=(c_{44}-c_{12})/c_{12}$.

	c_{11}	c_{12}	c_{44}	$c_{11}-c_{12}$	δ
Theory					
Present	395	205	220	190	0.07
Barker *et al.* ($T=0$ K)[a]					
(a) with ATM forces	416	232	228	186	−0.01
(b) without ATM forces	387	200	228	187	0.014
Experiment					
Neutron					
Fujii *et al.*[b]					
(a) Model 1	425±5	240±5	224±1	185±10	−0.07±0.02
(b) Sound speed	421±8	227±9	217±6	194±17	−0.04±0.05
Batchelder *et al.*[c]					
($T=4$ K)	411	190	210	221	0.11
Dorner and Egger[d]					
($T=4$ K)	367±14	174±17	234±11	193±31	0.34±0.12

[a] Reference 16.
[b] Force-constant model and sound speed obtained from fits to the same neutron data, Ref. 6.
[c] Reference 5.
[d] Reference 4.

The impact of including the three-body Axilrod-Teller-Muto forces can be seen clearly from the elastic constants listed in Table II. If we compare the calculations of Barker *et al.* with and without the ATM forces, we see the transverse branches controlled by c_{44} and $c_{11}-c_{12}$ are unaffected by including the ATM forces while c_{11} and c_{12} are increased by ~8% and ~14%, respectively. This means that while transverse phonons are unaffected by the ATM forces, the longitudinal frequencies are increased by ~4%. At high q this increase is reduced to 1–2% (M. L. Klein, private communication). The phonon frequencies calculated by Barker *et al.* and Klein *et al.* are essentially unchanged if the Bobetic-Barker pair potential is replaced by the Barker-Fisher-Watts pair potential.[18] The present elastic constants shown in Table II were calculated from the slope of the SCH + C phonon dispersion curves and have an estimated uncertainty of ±5 (10^8 dynes/cm^2).

From this we may conclude (a) that the phonon frequencies calculated using any of the modern realistic pair potentials and either quasiharmonic perturbation theory or self-consistent theory are essentially the same in Ar at low temperature, (b) that three-body forces increase the longitudinal frequencies by ~4% and are needed to get good agreement with experiment at low q (see Table II), and (c) there remains a small but definite disagreement at high q, with the calculated longitudinal frequencies lying 1–3% above the observed values. Since, as we shall see in Sec. V, the longitudinal groups at high q are already quite broad at $T=10$ K, it is not clear whether the disagreement arises from problems in establishing the one-phonon frequency accurately or whether there remains some physics in this disagreement. Otherwise, agreement with experiment verifies the pair potentials and suggests that the QHPT and SCH + C theories predict the frequencies equally well at $T \leq 10$ K.

IV. TEMPERATURE DEPENDENCE OF THE PHONON ENERGIES

The SCH + C phonon energy is defined in this section, as in the previous section, as the midpoint of the peak in $S(\vec{Q},\omega)$ of (2) at one-half the peak height. The SCH frequencies ω_{qj} are used in all the response functions that enter $S(\vec{Q},\omega)$. For the lower-energy phonons considered in this section this definition coincides with the definition as the position of the maximum in $S_1(\vec{Q},\omega)$. However, for some of the high-energy phonons discussed in the following section having a broad and somewhat asymmetric $S(\vec{Q},\omega)$, the midpoint at one-half the peak height can differ significantly from the position of the maximum in $S_1(\vec{Q},\omega)$. In addition, the two-phonon contribution has a significant energy dependence at higher energy making it difficult to separate the one-phonon component from the total $S(\vec{Q},\omega)$ if it were not calculated separately. In this case only a direct comparison of the total calculated $S(\vec{Q},\omega)$ with the observed scattering intensity is meaningful. To discuss phonon energies here we restrict ourselves, as did the experiments of Fujii

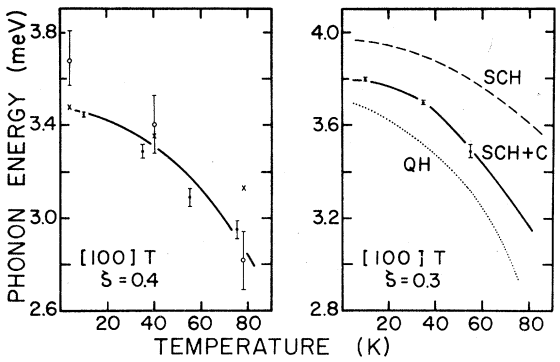

FIG. 3. Temperature dependence of the phonon energies. The solid and open points are from Fujii *et al.* (Ref. 6) and Batchelder *et al.* (Ref. 5), respectively. The crosses are the QHPT calculations of Klein *et al.* (Ref. 17) using the Bobetic-Barker (Ref. 15) pair potential.

et al., to lower-energy phonons where phonon energies can be meaningfully defined and where the one-phonon $S_1(\vec{Q},\omega)$ can be readily distinguished within the total $S(\vec{Q},\omega)$.

In Fig. 3 the SCH + C phonon energy for two transverse phonons is shown as a function of temperature. There we see that the temperature dependence of the SCH + C phonon energies agrees very well with the more recently observed values of Fujii *et al.* Also shown on the left-hand side of Fig. 3, as crosses, are the phonon energies calculated by Klein *et al.*[17] using the QHPT and the

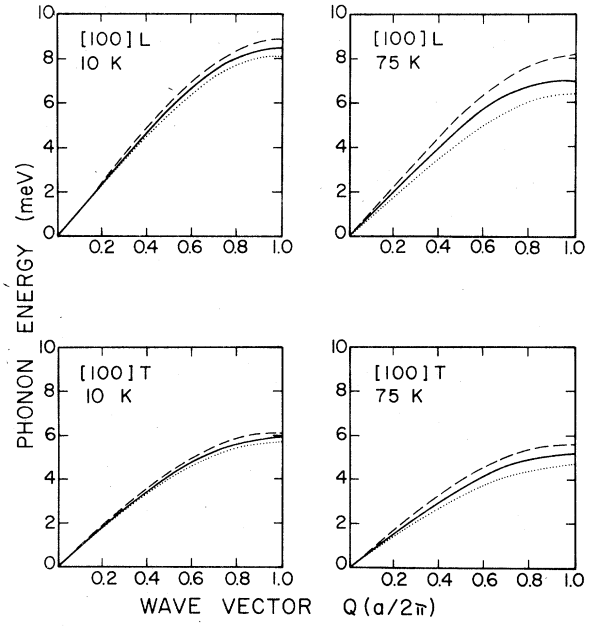

FIG. 4. The QH (····), the SCH (----), and the SCH+ C (——) phonon dispersion curves along the [100] direction at $T = 10$ and 75 K.

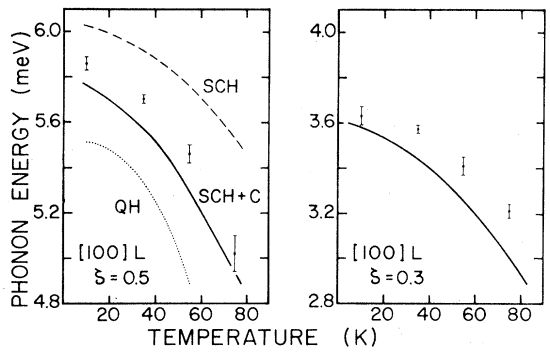

FIG. 5. Temperature dependence of longitudinal phonon energies along the [100] direction.

Bobetic-Barker potential which do not agree so well with experiment. We believe the difference between their energies at higher temperatures and the present SCH + C values represent the difference between the SCH + C and QHPT rather than a difference in the potential for the following reasons. Firstly, as shown in Fig. 1, the model realistic potentials do not differ substantially in the well region. Secondly, the phonon energies at low temperature are insensitive to these small differences as noted in Sec. III, particularly the transverse branch along the [100] direction (see Table I). Thirdly, we have calculated the cubic anharmonic shift in the QHPT and found it to be substantially different at high temperature from the same shift in the SCH + C theory. For these reasons we believe the SCH + C theory is a substantial improvement over the QHPT at high temperatures. The differences between the QH, the SCH, and the SCH + C frequencies at 10 and 75 K are shown in Fig. 4.

The temperature dependence of two longitudinal phonon energies is shown in Fig. 5. There we see that, while the SCH + C energies lie below the observed values at all temperatures, owing to the neglect of ATM forces, the temperature dependence

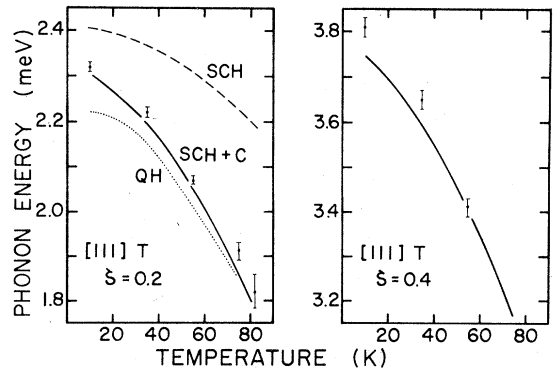

FIG. 6. Temperature dependence of transverse phonon energies along the [111] direction.

TABLE III. Elastic constants c_{ij} of Ar at $T=82$ K in 10^8 dynes/cm^2, $\delta=(c_{44}-c_{12})/c_{12}$.

	c_{11}	c_{12}	c_{44}	$c_{11}-c_{12}$	δ
Theory					
Present	220	135	115	85	−0.015
Klein and Murphy ($T=80$ K)[a]	250	163	119	87	−0.027
Fisher and Watts ($T=80$ K)[b]	244	161	112	83	−0.030
Gibbons *et al.* ($T=80$ K)[c]	237	157	112	80	−0.029
Experiment					
Neutron[d]	248±6	153±5	124±4	95±11	−0.019±0.04
Brillouin[e]	238±4	156±3	112±3	82±7	−0.028±0.04

[a] Bobetic-Barker potential, Ref. 15;
[b] Barker-Fisher-Watts potential, Ref. 34;
[c] Parson-Siska-Lee potential, Ref. 35, all including Axilrod-Teller-Muto three-body forces.
[d] Fujii *et al.*, Ref. 6.
[e] Gewurtz and Stoicheff, Ref. 36.

agrees will with experiment. A final example is shown in Fig. 6. These comparisons show the temperature dependence of the phonon energies can be calculated quite accurately using the SCH + C approximation.

In Table III are listed the elastic constants of Ar at $T=82$ K. There we see the present SCH + C c_{44} and $c_{11}-c_{12}$ agree well with previous values and experiment, but the c_{11} and c_{12} are too small owing to neglect of the three-body ATM forces. The neutron data represent zero-sound elastic constants and lie slightly above the first-sound Brillouin values. Clearly, ATM forces are needed to get agreement with experiment. The good agreement between the theory including these forces and experiment represents a triumph of both theory and experiment.

V. DYNAMIC FORM FACTOR

In this section we present calculations of the dynamic form factor $S(\vec{Q},\omega)$ of Eq. (2) using the SCP theory. This is done in two approximations. In the first the cubic anharmonic shift $\Delta(\vec{q}\lambda,\omega)$ and one-phonon damping $\Gamma(\vec{q}\lambda,\omega)$ are calculated simply as perturbations to the SCH frequencies. That is the averaged cubic force constant, Δ, Γ, $S_{12}(\vec{Q},\omega)$, and $S_2(\vec{Q},\omega)$ are all evaluated using the SCH frequencies. The SCH phonons are the "intermediate propagator" phonons in $S(\vec{Q},\omega)$. It was this approximation that was used to obtain the SCH + C frequencies of the previous section.

In the second approximation the SCH + C frequencies are used as the intermediate frequencies in $\Gamma(\vec{q}\lambda,\omega)$, $S_{12}(\vec{Q},\omega)$, and $S_2(\vec{Q},\omega)$. The second approximation simulates the first iteration in a fully self-consistent theory including the cubic anharmonic term. The cubic anharmonic force constant was not, however, reevaluated, and to keep the one-phonon response peak position consistent with the SCH + C frequencies defined above, the $\omega^2_{q\lambda}+2\omega_{q\lambda}\Delta(\vec{q}\lambda,\omega)$ was set at $\omega^2_{\mathrm{SCH+C}}$ in $A(\vec{q}\lambda,\omega)$. The aim of the second approximation is the use of the SCH + C frequencies which are the best estimate here of the true argon-crystal frequencies in Γ, $S_{12}(\vec{Q},\omega)$, and $S_2(\vec{Q},\omega)$ to get a more realistic value for the width of the phonon group and the contribution of $S_{12}(\vec{Q},\omega)$ and $S_2(\vec{Q},\omega)$ to $S(\vec{Q},\omega)$ in (2). Setting $\omega^2_{q\lambda}+2\omega_{q\lambda}\Delta(\vec{q}\lambda,\omega)=\omega^2_{\mathrm{SCH+C}}$ will be valid if $\Delta(\vec{q}\lambda,\omega)$ is not a very sensitive function of ω. The $S(\vec{Q},\omega)$ was folded with a Gaussian of FWHM of 0.4 meV (0.5 meV) for transverse (longitudinal) phonons to simulate the neutron scattering instrument-

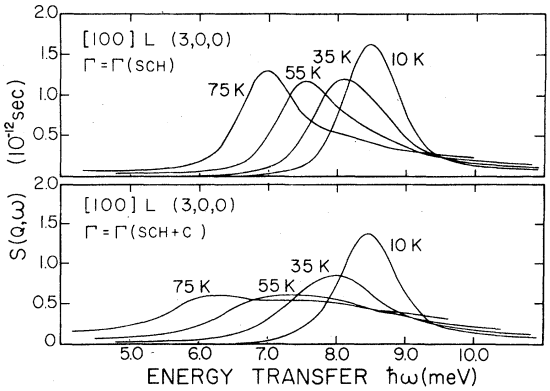

FIG. 7. Dynamic form factor, $S(\vec{Q},\omega)$, for the longitudinal phonon of wave vector $\vec{Q}=(2\pi/a)(3.0,0,0)$. The upper (lower) curve uses the SCH (SCH+C) frequencies in $\Gamma(\vec{q}\lambda,\omega)$ and $S_2(\vec{Q},\omega)$.

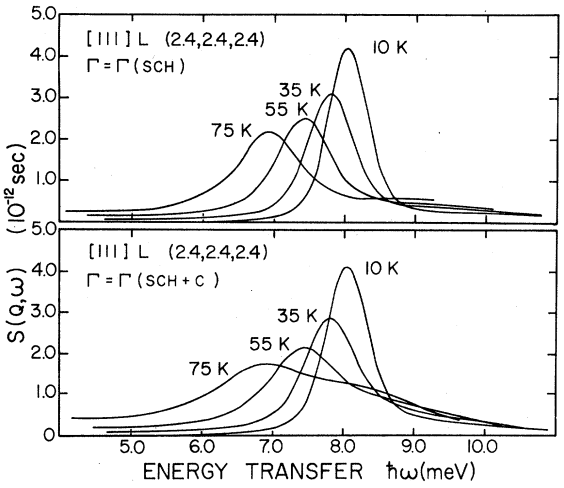

FIG. 8. As Fig. 7 for $\vec{Q}=(2\pi/a)$ (2.4, 2.4, 2.4).

al resolution width.

The $S(\vec{Q},\omega)$ for two high-frequency, longitudinal phonons having reduced wave vectors near the Brillouin-zone edge are displayed in Figs. 7 and 8. The one-phonon groups for these phonons are already broad at $T=10$ K. At $T=75$ K we see the one-phonon peak is dispersed over a very wide frequency range. It also depends very sensitively on whether the SCH or SCH + C frequencies are used in the one-phonon width $\Gamma(q\lambda,\omega)$ and $S_2(\vec{Q},\omega)$. Since the SCH + C frequencies are lower than the SCH frequencies the Γ(SCH + C) and S_2(SCH + C) lie in a lower-frequency range than Γ(SCH) and S_2(SCH). It turns out that this lowering means that Γ(SCH + C) and S_2(SCH + C) become substantially larger in the one-phonon peak energy range than the Γ(SCH) and S_2(SCH). This is true only for the high-energy phonons. The lower-energy phonons lie in an energy range below where either Γ(SCH + C) or Γ(SCH) are substantial.

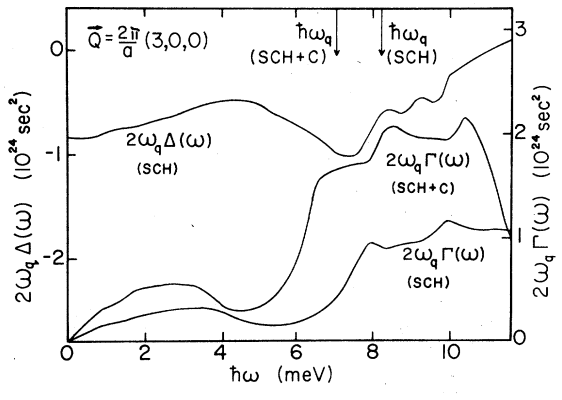

FIG. 9. Functions $2\omega_{q\lambda}\Delta(\vec{q}\lambda,\omega)$ and $2\omega_{q\lambda}\Gamma(\vec{q}\lambda,\omega)$ calculated with the SCH phonons as the intermediate propagator frequencies and $2\omega_{q\lambda}\Gamma(\vec{q}\lambda,\omega)$ calculated with SCH + C phonons as the propagator frequencies.

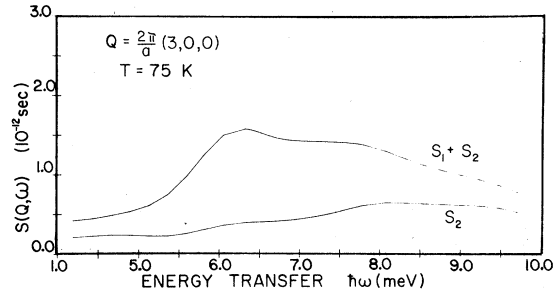

FIG. 10. Contribution of $S_2(\vec{Q},\omega)$ to $S_1(\vec{Q},\omega)+S_2(\vec{Q},\omega)$ for the longitudinal phonon at $\vec{Q}=(2\pi/a)$ (3,0,0) at $T=75$ K. For this phonon $S_{12}(\vec{Q},\omega)=0$.

This is displayed in Fig. 9 which shows Γ(SCH) and Γ(SCH + C) as well as Δ(SCH) for the longitudinal phonon at $\vec{Q}=(2\pi/a)$ (3, 0, 0).

The contribution of $S_2(\vec{Q},\omega)$ to the total $S(\vec{Q},\omega)$ for the longitudinal phonon at $\vec{Q}=(2\pi/a)$ (3.0, 0, 0) is shown in Fig. 10. There we see that $S_2(\vec{Q},\omega)$ is largely responsible for the large shoulder on the high-energy side of $S(\vec{Q},\omega)$. Since this $\vec{Q}$ lies midway between the two reciprocal-lattice vectors the interference term $S_{12}(\vec{Q},\omega)$ vanishes by symmetry for this phonon. The individual contributions of $S_{12}(\vec{Q},\omega)$ and $S_2(\vec{Q},\omega)$ to $S(\vec{Q},\omega)$ for the longitudinal phonon at $\vec{Q}=(2\pi/a)$ (2.4, 2.4, 2.4) are shown in Fig. 11. There we see the interference term is important for these high-energy phonons. However, in general the interference terms were significantly smaller in argon than in neon[30] and helium[25,31,33] where they are very substantial.

The $S(\vec{Q},\omega)$ for a lower-energy longitudinal phonon is shown in Fig. 12. There we see the $S(\vec{Q},\omega)$ is relatively insensitive to whether the SCH or SCH + C frequencies are used as the intermediate propagator frequencies. These $S(\vec{Q},\omega)$ may be compared directly with the observed groups of Fujii *et al.* shown in Fig. 13. There we see the calculated $S(\vec{Q},\omega)$ agrees well with the observed intensity except at $T=75$ K. The observed groups show

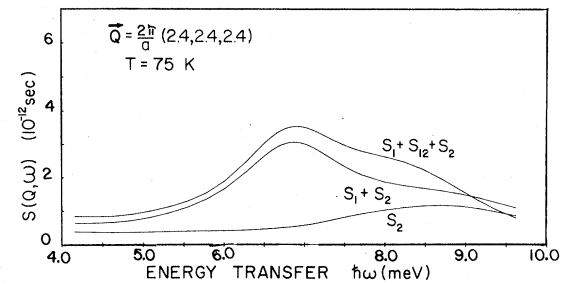

FIG. 11. Contributions of $S_2(\vec{Q},\omega)$ and $S_{12}(\vec{Q},\omega)$ to $S_1(\vec{Q},\omega)+S_{12}(\vec{Q},\omega)+S_2(\vec{Q},\omega)$ for the longitudinal phonon at $\vec{Q}=(2\pi/a)$ (2.4, 2.4, 2.4) at $T=75$ K.

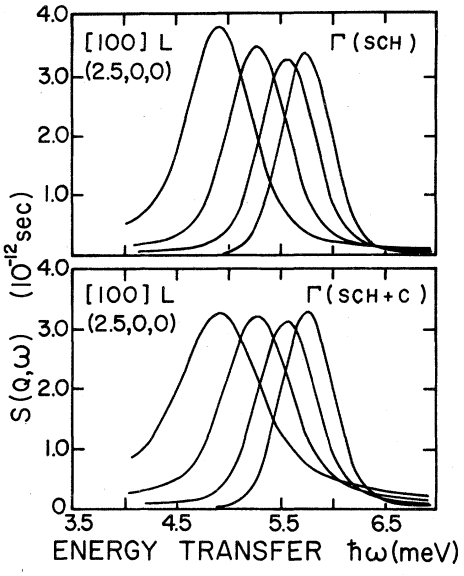

FIG. 12. As Fig. 7 for $\vec{Q}=(2\pi/a)$ (2.5,0,0).

a very abrupt broadening between 55 and 75 K not reproduced by the theory. Finally, the temperature dependence of the phonon groups for some transverse phonons are shown in Fig. 14.

Generally, the groups for phonons having energies ≤ 6 meV were symmetrical, "well behaved," and insensitive to whether the SCH or SCH + C frequencies were used as intermediate propagator

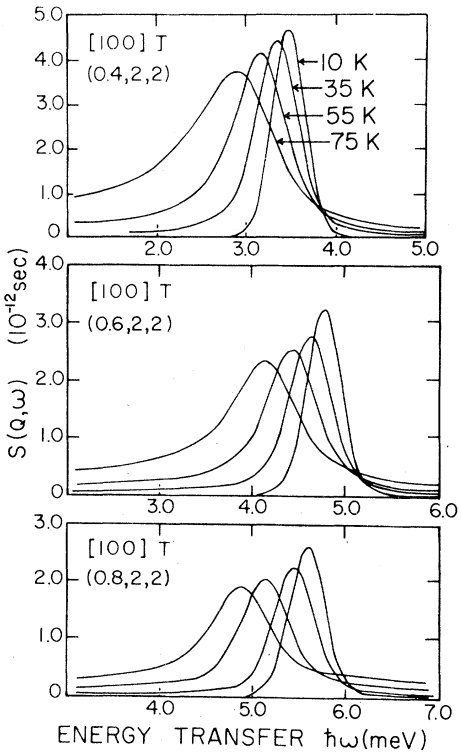

FIG. 14. Dynamic form factors for transverse phonons along the [100] direction using the SCH+C frequencies in $\Gamma(\vec{q}\lambda,\omega)$, $S_{12}(\vec{Q},\omega)$, and $S_2(\vec{Q},\omega)$.

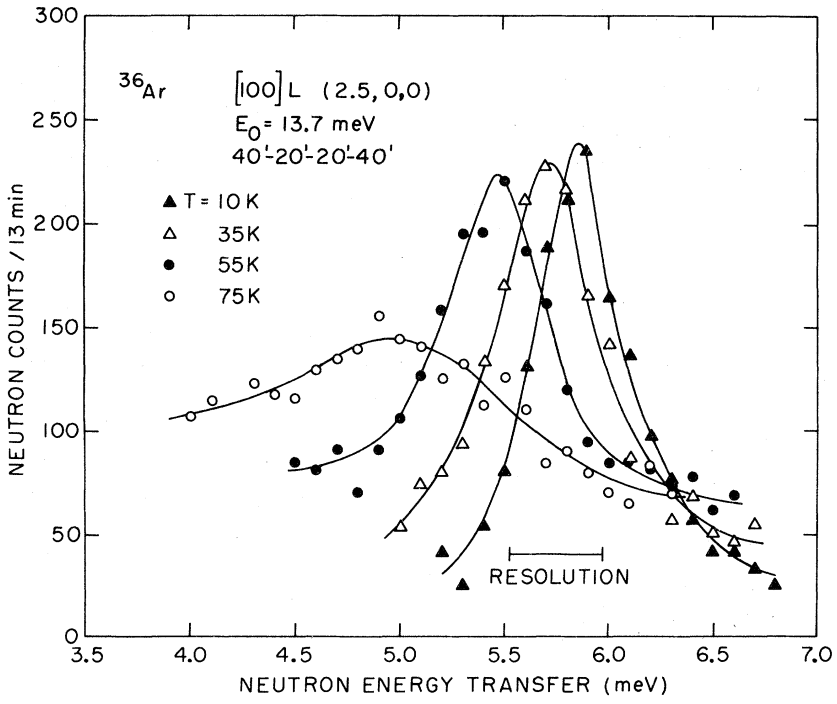

FIG. 13. Phonon groups observed by Fujii *et al.* (Ref. 6) for comparison with Fig. 12.

frequencies. For higher-energy phonons ($\hbar\omega \gtrsim 6$ meV, $S_1(\vec{Q},\omega)$ is broad and peaks in the energy range where $\Gamma(\vec{q}\lambda,\omega)$ and $S_2(\vec{Q},\omega)$ are rapidly increasing (see Figs. 9 and 10) leading to a plateau on the high-energy side of $S(\vec{Q},\omega)$. For these phonons $S(\vec{Q},\omega)$ is very sensitive to whether the SCH or SCH + C frequencies are used as intermediate propagator frequencies. In a fully self-consistent, second-order theory the frequencies given by the mean position of the phonon group should be used. For the higher-energy phonons having a high-frequency tail this mean frequency will be larger than the SCH + C frequency. Thus, using the SCH + C frequencies will tend to overestimate the effect of changing the intermediate frequencies. The purpose here is to show that for $\hbar\omega \gtrsim 6$ meV the group widths are sensitive to the intermediate frequencies. A definitive group shape will have to await a fully self-consistent theory which would have to include short-range correlations.

VI. COMPARISON WITH MOLECULAR DYNAMICS

Using the method of molecular dynamics (MD) it is now possible to simulate classical liquids and solids directly. In this method Newton's equations of motion are solved numerically for N atoms in a volume V to evaluate the atomic positions $\vec{r}_l(t) = \vec{R}_l + \vec{u}_l(t)$ as a function of time. With this information properties such as the dynamic form factor $S(\vec{Q},\omega)$ in (1) can be calculated directly. Within the accuracy of the method, the resulting $S(\vec{Q},\omega)$ should be exact, including all anharmonic contributions. Thus a comparison of $S(\vec{Q},\omega)$ calculated using the SCP theory with MD should provide a test of the theory.

In an interesting study, Hansen and Klein have simulated the rare-gas solids using MD, assuming the rare-gas atoms interact via the Lennard-Jones potential

$$v(r) = 4\epsilon[(\sigma/r)^{12} - (\sigma/r)^6],$$

where for ^{36}Ar $\sigma = 3.405$ Å and $\epsilon = 119.8$ K. This potential is compared with the more realistic potentials in Fig. 1. To make direct comparison with their simulation we have calculated $S(\vec{Q},\omega)$ using the Lennard-Jones potential in ^{36}Ar at densities and temperatures considered by them.

In Fig. 15, the $S(\vec{Q},\omega)$ for the longitudinal phonon having wave vector $\vec{Q} = (2\pi/a)\,(0.5, 0, 0)$ in ^{36}Ar at $T = 39.5$ K ($a = 5.3521$) and $T = 87.5$ K ($a = 5.4603$) calculated here using the SCH + C theory and by Hansen and Klein using the MD method are compared. Both $S(\vec{Q},\omega)$ are folded with a Gaussian, of FWHM = 0.22 in the MD case and of FWHM = 0.4 meV in the SCH + C case. In this calculation the Lennard-Jones potential was truncated after the

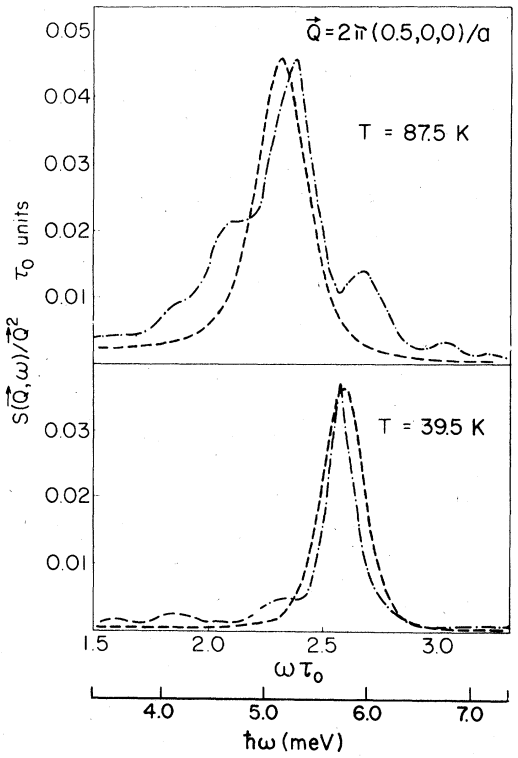

FIG. 15. $S(\vec{Q},\omega)$ for the longitudinal phonon halfway to the zone boundary in the [100] direction (Lennard-Jones potential) — — SCH+C, —— – —— MD.

first-neighbor shell. For more direct comparison the SCH + C theory $S(\vec{Q},\omega)$ was multiplied by a single scale factor of 1.18 at both temperatures so that at $T = 39.5$ K the two $S(\vec{Q},\omega)$ lie directly on top of one another. Without this factor the SCH + C $S(\vec{Q},\omega)$ would lie somewhat below the MD $S(\vec{Q},\omega)$, perhaps due to multiphonon contribution not included in the SCH + C $S(Q,\omega)$. The temperature $T = 87.5$ K lies slightly above the melting point ($T = 84$ K).

From Fig. 15 we see that the peak positions of the $S(\vec{Q},\omega)$ agree well, particularly the change of this peak position with temperature. The increase in the width and intensity of $S(\vec{Q},\omega)$ with temperature also agrees well. Thus except for the humps on the MD $S(\vec{Q},\omega)$, which may be due to statistical noise, the SCH + C $S(\vec{Q},\omega)$ reproduces the MD results well. This phonon group, calculated using the Aziz-Chen potential and observed by Fujii *et al.*, is also shown in Figs. 12 and 13, respectively. Since the SCH + C $S(\vec{Q},\omega)$ in Fig. 12 peaks at energies slightly below but in a good agreement with the observed peaks in Fig. 13, the MD and experiment phonon group peaks are consistent. The observed group at $T = 75$ K in Fig. 13 is substantially broader than would be predicted by MD

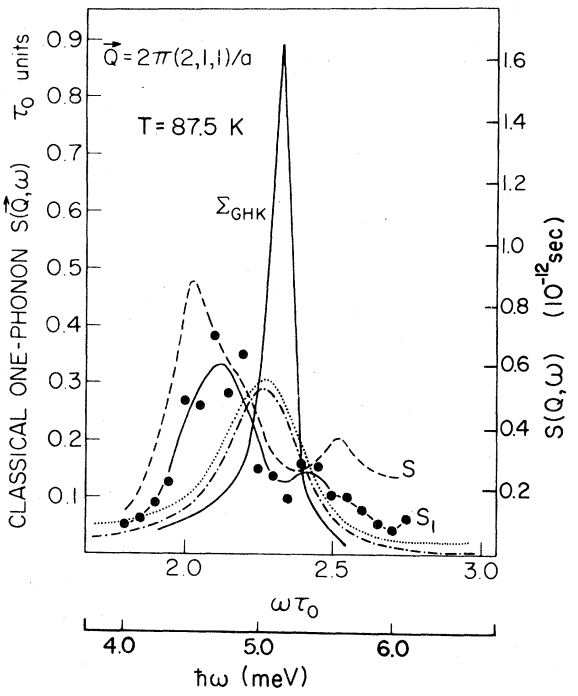

FIG. 16. The one phonon, S_1, and full S for the transverse phonon on the zone boundary in the [100] direction at $T = 87.5$ K. The dots and solid line are S_1 by MD, dashed line S by MD. The dashed (dotted) lines are S (S_1) calculated here using the Lennard-Jones potential and the SCH+C theory. The peaked line is an SCP $S(\vec{Q},\omega)$ calculated without folding by Goldman (as in Ref. 39).

simulation.

In Fig. 16 a similar comparison is made for the transverse phonon having wave vector $\vec{Q} = (2\pi/a)$ (2, 1, 1) [equivalent to a reduced $\vec{q} = (2\pi/a)$ (1, 0, 0) at $T = 87.5$ K]. In this case the Lennard-Jones potential was truncated after three neighbor shells. The two $S(\vec{Q},\omega)$ are plotted in the unadjusted units noted in the figure. While the intensity and width of the SCH + C theory $S(\vec{Q},\omega)$ and $S_1(\vec{Q},\omega)$ compares well with the MD results, the SCH + C $S(\vec{Q},\omega)$ peaks at much higher energy. This disagreement in peak position is surprising since the peak position of the SCH + C theory $S(\vec{Q},\omega)$ for the T[100] branch calculated using the Aziz-Chen potential agreed extremely well with experiment at all temperatures, as shown in Fig. 3. Regarding the SCH + C theory as an interpolation scheme to connect the MD simulation and experiment suggests the MD peak position would not agree with experiment in this case.

From Figs. 15 and 16 we conclude that the width and shape of the SCH + C theory $S(\vec{Q},\omega)$ agree well with the MD simulation near melting in ^{36}Ar, although the peak position does not always agree well.

VII. DISCUSSION

In the previous sections we saw that the SCH + C theory predicts phonon frequencies in good agreement with experiment right up to 82 K. The values obtained are much improved over those predicted by QHPT. For low-frequency phonons, where comparison with experiment is possible, the phonon lifetimes and shape of $S(Q,\omega)$ are also quite well predicted (see Figs. 12 and 13). These shapes are also reasonably insensitive to how $S(\vec{Q},\omega)$ is calculated. In addition, the Aziz-Chen potential, which describes gas and liquid-argon properties precisely, clearly predicts the phonon properties well although the phonon data are not really precise enough to distinguish between the Aziz-Chen and Barker-Fisher-Watts potentials, for example.

With the above positive points we recall that the $S(\vec{Q},\omega)$ for the high-frequency, longitudinal phonons predicted by the SCH + C theory are very broad and very sensitive to the values used for the intermediate propagator frequencies at $T \gtrsim 55$ K (e.g., see Figs. 7 and 8). This is both because $S_1(\vec{Q},\omega)$ itself is very broad and because $S_1(\vec{Q},\omega)$ falls in a frequency range where $S_2(\vec{Q},\omega)$ is rapidly increasing with ω. For these reasons a fully self-consistent theory including the cubic anharmonic term is required to establish $S(\vec{Q},\omega)$ for high-frequency phonons precisely. This fully self-consistent theory should also include recalculating the averaged harmonic and cubic force constants at each stage of the iteration.

It is also clear both from experiment and theory that $S(\vec{Q},\omega)$ for high-frequency phonons in ^{36}Ar at $T \gtrsim 55$ K is indeed very broad. A similarly broad $S(\vec{Q},\omega)$, having a plateau on the high-frequency side due to a rapidly rising $S_2(\vec{Q},\omega)$, was found for high-frequency phonons in fcc He[33] and Ne.[37] However, the $S_1(Q,\omega)$ appears to be even broader in Ar near melting than in Ne, fcc ^{4}He or even in the more quantum hcp and bcc phases of helium.[38] The $S_1(Q,\omega)$ is broad for high-energy phonons in Ar because $S_1(\vec{Q},\omega)$ lies in a frequency range where $\Gamma(\vec{q},\omega)$ is large (see Fig. 9). In bcc He, for example, $S_1(\vec{Q},\omega)$ always lies in a frequency range below which the corresponding $\Gamma(\vec{q},\omega)$ becomes large (see Fig. 4, Ref. 40). Thus the phonons are broader in Ar due to the closer relative positions of $S_1(\vec{Q},\omega)$ and $\Gamma(\vec{q},\omega)$ in Ar rather than to larger intrinsic anharmonic effects. Thus, although the quantum phases of helium are the most anharmonic, the phonons have long lifetimes because the phonon energies are small and lie in a region where $\Gamma(\vec{q},\omega)$ is small. The rms vibrational amplitude in bcc ^{4}He is ~30–35 % of the interatomic spacing compared to 15–18 % in Ar at the triple point.

Finally, would a theory including an explicit description of short-range correlations improve agreement with experiment? Certainly, including short-range correlations changes the force constants and in that sense they are important.[41-43] Also, the SCH + C theory is an improvement over the QHPT largely because the initial SCH frequencies are closer to the observed values and the subsequent cubic frequency shift is smaller; that is, the SCH frequencies are a better basis. If including short-range correlations provides a still better basis, then improvement can be expected. In this case the cubic anharmonic term would be further reduced. Experience in solid helium shows that this reduction in the cubic coefficient $\langle\nabla(0)\nabla(0)\nabla(l)v(r_{0l})\rangle$, when short-range correlations are included, substantially lengthens the phonon lifetime. Since experiment and MD tend to confirm that the phonon lifetimes in Ar are indeed short, incorporating short-range correlations should not change the averaged force constants too dramatically. An experimental determination of $S(\vec{Q},\omega)$ for the high-energy phonons in Ar would therefore be most interesting as a critical test of future theories.

ACKNOWLEDGMENTS

It is a pleasure to acknowledge valuable discussions with Dr. G. K. Horton, Dr. M. L. Klein, and Dr. J. Eckert.

[1]G. K. Horton, in *Rare Gas Solids*, edited by M. L. Klein and J. A. Venables (Academic, New York, 1976), Vol. I, Chap. 1.
[2]J. A. Barker, in *Rare Gas Solids*, edited by M. L. Klein and J. A. Venables (Academic, New York, 1976), Vol. I, Chap. 4; B. M. Axilrod and E. Teller, J. Chem. Phys. 11, 299 (1943); Y. Muto, Proc. Phys. Math. Soc. Jpn. 17, 629 (1943).
[3]W. B. Daniels, G. Shirane, B. C. Frazer, H. Umebayashi, and J. A. Leahe, Phys. Rev. Lett. 19, 1307 (1967).
[4]H. Egger, M. Gsänger, E. Lüscher, and B. Dorner, Phys. Lett. A28, 433 (1968).
[5]D. N. Batchelder, M. F. Collins, B. C. G. Haywood, and G. R. Sidey, J. Phys. C 3, 249 (1970).
[6]Y. Fujii, N. A. Lurie, R. Pynn, and G. Shirane, Phys. Rev. B 10, 3647 (1974).
[7]E. R. Dobbs and G. O. Jones, Rep. Prog. Phys. 20, 516 (1957).
[8]G. K. Pollack, Rev. Mod. Phys. 36, 748 (1964).
[9]G. Boato, Cryogenics 4, 65 (1964).
[10]E. A. Guggenheim, *Applications of Statistical Mechanics* (Clarendon, Oxford, 1966).
[11]G. K. Horton, Am. J. Phys. 36, 93 (1968).
[12]G. K. Horton and J. W. Leech, Proc. Phys. Soc. London 82, 816 (1963).
[13]L. Bohlin and T. Högberg, J. Phys. Chem. Solids 29, 1805 (1968).
[14]G. Niklasson, Phys. Condens. Matter 14, 138 (1972).
[15]M. V. Bobetic and J. A. Barker, Phys. Rev. B 2, 4169 (1970).
[16]J. A. Barker, M. L. Klein, and M. V. Bobetic, Phys. Rev. B 2, 4176 (1970).
[17]M. L. Klein, J. A. Barker, and T. R. Koehler, Phys. Rev. B 4, 1983 (1971).
[18]M. L. Klein and T. R. Koehler, in *Rare Gas Solids*, edited by M. L. Klein and J. A. Venables (Academic, New York, 1976), Vol. I, Chap. 6.
[19]J. A. Barker, R. A. Fisher, and R. O. Watts, Mol. Phys. 21, 657 (1971).
[20]V. V. Goldman, G. K. Horton, T. H. Keil, and M. L. Klein, J. Phys. C 3, L33 (1970).
[21]J. P. Hansen and M. L. Klein, Phys. Rev. B 13, 878 (1976).
[22]R. A. Aziz and H. H. Chen, J. Chem. Phys. 67, 5719 (1977).
[23]L. Van Hove, Phys. Rev. 95, 249 (1954); W. Marshall and S. W. Lovesey, *Theory of Thermal Neutron Scattering* (Oxford University, Oxford, 1971).
[24]R. A. Cowley, Adv. Phys. 12, 42 (1963); Rep. Prog. Phys. 31, 123 (1968).
[25]H. R. Glyde, Can. J. Phys. 52, 2281 (1974).
[26]P. F. Choquard, *The Anharmonic Crystal* (Benjamin, New York, 1967); T. R. Koehler, in *Dynamical Properties of Solids*, edited by G. K. Horton and A. A. Maradudin (North-Holland, Amsterdam, 1975), Vol. 2.
[27]T. R. Koehler, Phys. Rev. Lett. 22, 777 (1969); H. R. Glyde and M. L. Klein, Crit. Rev. Solid State Sci. 2, 181 (1971).
[28]V. Ambegaokar, J. Conway, and G. Baym, in *Lattice Dynamics*, edited by R. F. Wallis (Pergamon, New York, 1965), p. 261.
[29]R. A. Cowley and W. J. L. Buyers, J. Phys. C 2, 2262 (1969).
[30]L. Bohlin, Solid State Commun. 10, 1219 (1972).
[31]H. Horner, Phys. Rev. Lett. 29, 556 (1972).
[32]J. Meyer, G. Dolling, R. Schern, and H. R. Glyde, J. Phys. F 6, 943 (1976).
[33]W. M. Collins and H. R. Glyde, Phys. Rev. B 18, 1132 (1978).
[34]R. A. Fisher and R. O. Watts, Mol. Phys. 23, 1051 (1972).
[35]J. M. Parson, P. E. Siska, and Y. T. Lee, J. Chem. Phys. 56, 1511 (1972).
[36]S. Gewurtz and B. P. Stoicheff, Phys. Rev. B 10, 3487 (1974).
[37]W. M. Collins and H. R. Glyde, Phys. Rev. B 17, 2766 (1978).
[38]V. J. Minkiewicz, J. A. Kitchens, G. Shirane, and E. B. Osgood, Phys. Rev. A 8, 1513 (1973); J. Eckert, W. Thomlinson, and G. Shirane, Phys. Rev. B 16, 1057 (1977), W. Thomlinson, J. Eckert, and G. Shirane, *ibid.* 18, 1120 (1978); C. Stassis, G. Kline, W. A. Kamithakara, and S. K. Sinha, *ibid.* 17, 1130 (1978).
[39]V. V. Goldman, G. K. Horton, and M. L. Klein, Phys. Rev. Lett. 24, 1424 (1970).

[40]H. R. Glyde and F. C. Khanna, Can. J. Phys. 49, 2997 (1971).
[41]H. Horner, in *Dynamical Properties of Solids*, edited by A. A. Maradudin and G. K. Horton (North-Holland, Amsterdam, 1974), p. 450; and in *Proceedings of the IAEA Conference on Neutron Inelastic Scattering, Vienna, 1972* (IAEA, Vienna, 1972), p. 119.
[42]L. B. Kanney and G. K. Horton, Phys. Rev. Lett. 34, 1565 (1975).
[43]J. Leese and G. K. Horton (unpublished).